# Internally Tagged Ubiquitin: a Tool to Identify Linear Polyubiquitin-modified Proteins by Mass Spectrometry

Katarzyna Kliza[1], Christoph Taumer[2], Irene Pinzuti[3], Mirita Franz-Wachtel[2], Simone Kunzelmann[4], Benjamin Stieglitz[3], Boris Macek[2] & Koraljka Husnjak[1*]

[1]Institute of Biochemistry II, Goethe University School of Medicine, Germany. [2]Proteome Center Tuebingen, Tuebingen, Germany. [3]Department of Chemistry and Biochemistry, Queen Mary University of London, London, United Kingdom. [4]Structural Biology Science Technology Platform, Francis Crick Institute, London, United Kingdom.

Correspondence should be addressed to K.H. (husnjak@biochem2.de)

**Running Title:** A Novel Approach to Identifying Linear Polybiquitin Substrates

**Even though ubiquitination controls a plethora of cellular processes, modifications by linear polyubiquitin have so far only been linked with acquired and innate immunity, lymphocyte development and genotoxic stress response. Until now, a single E3 ligase complex (LUBAC), one specific deubiquitinase (OTULIN) and a very few substrates have been identified. The existing methods for the study of lysine-based polyubiquitination are not suitable for the detection of linear polyubiquitin-modified proteins. Here, we present a novel approach to discovering linear polyubiquitin-modified substrates by combining lysine-less internally tagged ubiquitin (INT-Ub.7KR) with SILAC-based mass spectrometry. We applied our approach in TNFα-stimulated T-REx HEK293T cells and afterwards validated newly identified linear polyubiquitin targets. Moreover, we demonstrated that linear polyubiquitination of the novel LUBAC substrate TRAF6 is essential for the NFκB signalling. Overall, we have established a powerful method for the detection of linear polyubiquitin substrates.**

Post-translational modification by ubiquitin (Ub) regulates fundamental cellular processes, including protein stability, DNA repair, inflammation and immune response[1,2]. Apart from mono- and multiple monoubiquitination, all 7 internal Ub lysine (K) residues can form K-specific Ub linkages, thus forming polyUb chains with distinct structures, assembly machineries and functions in the cell[3]. Additionally, the N-terminal methionine (M) of Ub can form a peptide bond with the terminal glycine (G) of another Ub moiety, generating linear polyUb chains[4].

Even though its basal cellular levels are very low[5,6], linear polyubiquitination can be rapidly induced in the cell, eliciting a specific cellular response to a given stimulus. These stimuli include TNFα[7], heat stress response[8] and bacterial infection[9], with linear polyubiquitination being crucial in inducing inflammatory, acquired and innate immune responses[10], genotoxic stress response and Parkinson´s disease[11]. Additionally, numerous cellular processes require timely regulated and coordinated activation of linear polyubiquitination, such as survival of mature T cells[12], late thymic T-cell differentiation[13] and B-cell development and activation[14] .

The only E3 ligase complex described so far to be able to generate linear polyUb chains is LUBAC (Linear Ubiquitin Assembly Complex) and consists of three proteins: catalytic subunit RNF31/HOIP[15,16], RBCK1/HOIL-1L and SIPL1/SHARPIN[17-19], whereas OTULIN (FAM105B or GUMBY) is the main deubiquitinating enzyme (DUB) highly specific for linear Ub chains[20,21].

Only a handful of linear polyUb-modified substrates has been identified so far[7,18,22-24], including K63-linked polyUb chains leading to the generation of mixed, K63/M1 hybrid polyUb linkages[25]. Nevertheless, these few proteins (including NEMO) have already been linked with several severe diseases, such as X-linked anhidrotic ectodermal dysplasia with immunodeficiency (XR-EDA-ID)[26-28], justifying the need for an approach allowing the identification of novel linear polyUb targets and related processes.

The most widely used approach for the identification of ubiquitinated proteins is Ub remnant profiling[29-31]. Unfortunately, GGK-specific monoclonal antibodies[29-31] do not recognise the characteristic GGMQIFVK signature peptides of linear polyubiquitination after tryptic cleavage. Additionally, the other existing methods have limitations for the identification of linear polyubiquitination substrates: a) N-terminally tagged Ub constructs[32-34] prevent linear polyUb chain assembly due to the requirement for a free M1 residue to build linear polyUb chain, b) the use of tandem linear polyUb-binding domains (UBDs) for the enrichment of linear polyUb chains is limited to mild cellular lysing conditions, leading to the high background in mass spectrometry (MS) analyses and resulting in a large number of false positive hits; an additional disadvantage of linear UBDs is that they can also bind K63-linked Ub chains to a certain extent, and c) the two currently available linear polyUb-specific antibodies are not optimal. The Genentech-generated antibody 1F11/3F5/Y102L can, to a certain extent, recognise and capture K63-linked polyUb chains[5], while the Lub9 antibody is not suitable for immunoprecipitation (IP) experiments, thus limiting its applicability only to confirmation of already identified linear polyUb targets[14].

We describe herein a novel approach for the specific enrichment of linear polyUb-modified substrates, which enabled the identification of novel linear polyUb targets, including ATR, BRAP, LGALS7, PLAA, SEPT2, HDAC6, VDAC1 and TRAF6. Moreover, we could demonstrate that linear polyubiquitination of TRAF6 is essential for proper IL1β-dependent NFκB signalling.

## RESULTS

**Generation of INT-Ub for the Study of Linear Polyubiquitination.** As an internal tag within Ub we chose STREP-tag® II, flanked on each side by the short serine-alanine (SA) linker, which was incorporated instead of arginine 54 (R54) residue of Ub (Figure 1A). We chose STREP-tag® II because this short, almost biochemically inert tag strongly interacts with the engineered streptavidin Strep-Tactin®, even under denaturing conditions. Since internally tagged Ub (INT-Ub) can build any type of polyUb chain, we also generated INT-Ub, having all 7 K residues replaced by R (INT-Ub.7KR). Even though this INT-Ub.7KR variant can also monoubiquitinate target proteins and add terminal Ub moiety to any type of polyUb chains, it can be efficiently incorporated at multiple positions only within a single Met1-linked polyUb chain, thus enabling the enrichment of linear polyUb-modified proteins (Supplementary Figure 1A).

**Evaluation of INT-Ub Functionality *in vitro.*** To determine the functionality of INT-Ub, we investigated if the presence of the internal tag affected the main structural and functional features of Ub. We used NMR spectroscopy (Figure 1B) and circular dicroism (Supplementary Figures 1B-1C) to validate the structural integrity of INT-Ub. In all of our measurements INT-Ub variants display highly similar spectra compared to wild-type Ub, indicating that the secondary and tertiary structures of the recombinant INT-Ub are almost identical to wild-type Ub. Therefore, the overall fold of Ub is not compromised by the internal tag. We could also demonstrate that recombinant INT-Ub, unlike unconjugatable INT-Ub.ΔGG mutant, can form various polyUb chains (Figure 1C, Supplementary Figures 1D-1E). Additionally, INT-Ub can bind UBDs that recognise single Ub moieties (Supplementary Figure 1F), with the internal tag also not affecting the ability of linear diUb to bind to linear polyUb-specific UBD UBAN (Ubiquitin binding in ABIN and NEMO)[35] (Figure 1D and Supplementary Figure 1G). Moreover, recombinant INT-diUb could be cleaved by Ub chain-unspecific DUB fragment USP2-cc (Figure 1E)[36] and linear polyUb-specific DUB OTULIN (Figure 1F, Supplementary Figures 1H-1I).

**Evaluation of INT-Ub Functionality *in vivo.*** As INT-Ub was shown to be functional *in vitro*, we next evaluated its functionality *in vivo*. Towards that aim, we generated T-REx HEK293T and T-REx HeLa cell lines inducibly expressing low amounts of wild-type INT-Ub, INT-Ub.7KR or INT-Ub.ΔGG mutant, in order to ensure the presence of INT-Ub variants only as minor fractions of the total cellular Ub pool (Supplementary Figure 2A). As shown in Figure 2A, high molecular weight (HMW) Ub species, indicative of polyubiquitinated substrates, were visible in the case of INT-Ub and INT-Ub.7KR, contrary to INT-Ub.ΔGG.

Taking advantage of the STREP-tag® II position between residues K48 and K63, we identified GG-K48-INT-Ub and GG-K63-INT-Ub peptides in the INT-Ub sample by MS approach, confirming the INT-Ub presence within polyUb chains *in vivo* (Figure 2B). Moreover, we could demonstrate that pulled-down INT-Ub, unlike INT-Ub.ΔGG, is enriched in ubiquitinated substrates by detecting endogenous PAF15 (PCNA Associated Factor 15), which is known to be mono- and double monoubiquitinated[37] (Figure 2C). Another important aspect to rule out was if INT-Ub variants, particularly INT-Ub.7KR, perturb cellular functions. As a model process, we chose the NFκB signalling pathway, since it is highly regulated by ubiquitination, with linear polyubiquitination of NEMO being crucial for NFκB activation[7,18]. Upon TNFα stimulation, expression of INT-Ub variants did not affect nuclear translocation of NFκB dimers compared to the empty vector control (Figures 2D-E). Additionally, we did not observe any significant difference in the transcriptional activity of NFκB in any cell line, except for INT-Ub.ΔGG (Figure 2F and Supplementary Figure 2B). Therefore, we concluded that the stable cell lines inducibly expressing INT-Ub variants were appropriate for further *in vivo* studies.

Finally, we induced the formation of linear polyUb chains in cells by several approaches: transient transfection of OTULIN siRNA (Figure 3A), catalytic-inactive OTULIN mutant C129A (Figure 3B) or HOIP/HOIL-1L (Figure 3C), as well as TNFα treatment (Figure 3D) in doxycycline-induced INT-Ub.7KR T-REx HEK293T cells. In all the cases, the amount of pulled-down HMW Ub species was increased compared to control conditions (Figure 3A-D). Furthermore, samples with transiently transfected OTULIN C129A mutant had increased amounts of HMW STREP-tag® II-containing species, indicating the enrichment of INT-Ub.7KR (Figures 3E). To verify that the HMW Ub species indeed contained linear polyUb, samples were immunoblotted with the Lub9 antibody (Figure 3F and Supplementary Figure 2C), further confirming the presence of linear polyUb-modified substrates. Moreover, we could demonstrate the presence of HMW species of the known LUBAC substrate NEMO in INT-Ub.7KR PD (Supplementary Figure 2D) upon TNFα treatment, confirming that INT-Ub.7KR enables enrichment of linear polyUb-modified proteins.

**Identification of Novel Linear Polyubiquitin Targets.** For our MS screen, we chose TNFα stimulation as the well-established physiological stimulus[7,38] for the induction of linear polyubiquitination (Figure 4A and Supplementary Figure 3A). For the initial MS experiment, cells were treated with TNFα for 15 min (Supplementary Table 1). Due to the relatively low SILAC ratios in the MS screen (Supplementary Figure 3B), we further optimised the procedure by modifying lysis/PD buffer, by replacing Strep-Tactin® with the third generation

of Strep-Tactin® XT resins (IBA), as well as by generating a new set of SILAC-labelled T-REx HEK293T cell lines expressing INT-Ub variants. Moreover, the time of TNFα stimulation was decreased to 10 min, for optimal induction of linear polyubiquitination[39]. During MS measurements of three independent experimental replicates, a total of 1,695 protein groups were quantified at FDR of 1% at protein and peptide level (Supplementary Table 2). Correlation of measured SILAC ratios was high between replicates of INT-Ub/INT-Ub.ΔGG and INT-Ub/INT-Ub.7KR (Pearson Correlation Coefficient 0.77-0.85; Supplementary Figure 3C). Correlation was lower between replicates of INT-Ub.7KR/INT-Ub.ΔGG (Pearson Correlation Coefficient 0.36-0.45), which may be attributed to a lower number of significantly changing ratios and explained by the fact that linear polyubiquitination is a very rare cellular event. As expected, KEGG and GOMF annotation enrichment analyses showed significant over-representation of Ub-related processes and proteins, further confirming that INT-Ub variants are functional (Figure 4B-C). Interestingly, protein functions related to systemic lupus erythematosus, an autoimmune disease recently linked with linear polyubiquitination and LUBAC[40], were significantly enriched. Moreover, the MS dataset showed statistically significant overrepresentation of proteins linked with Parkinson's disease. PARKIN has already been linked with inflammation and shown to interact with LUBAC to regulate both LUBAC activity[41] and its recruitment to the mitochondria, resulting in abrogated IFNβ production[42]. Therefore, KEGG enrichment analysis indirectly suggests that the MS dataset was indeed enriched in linear polyUb-modified proteins. The putative linear polyUb-modified substrate selection was focused on proteins preferentially present in INT-Ub (L) and INT-Ub.7KR (M) SILAC-labelled inducible T-REx HEK293T cells, in comparison to INT-Ub.ΔGG (H) SILAC-labelled cells (which were used as a negative MS control) (Figure 4D and Supplementary Table 2). Since both INT-Ub and INT-Ub.7KR could be incorporated into linear polyUb chains, INT-Ub/INT-Ub.7KR (L/M) ratio was considered as the supporting selection criterion. For the validation of the INT-Ub approach, we chose several candidates with SILAC ratios equal or above 2, such as ATR, BRAP, LGALS7 and PLAA. To test the sensitivity of our method, we also included several proteins found near MS background in both preliminary and triplicate MS experiments, such as SEPT2, HDAC6, VDAC1 and TRAF6 (the latter protein was identified only in the preliminary MS screen, due to much lower expression level in the second set of T-REx HEK293T cell lines (Supplementary Figure 3D).

**Validation of Putative Linear Polyubiquitin-modified Substrates.** Since there is no well-established method for the confirmation of protein modification by linear polyUb, we

performed several complementary approaches to validate novel substrates. For our MS screens we used TNFα to induce linear polyubiquitination. We therefore reasoned that, even if additional, unidentified linear polyUb-specific E3 ligases exist in the cell, we would preferentially identify LUBAC-dependent substrates.

First, for the majority of them, we could show HMW species migrating above protein bands, both on total cell lysate (TCL) level and upon IP, only in the presence of the active LUBAC complex, indicative of (presumably linear) polyubiquitination. No HMW species were observed when catalytic-dead LUBAC (HOIP C885A/HOIL-1L) was used (Supplementary Figure 4A, and data not shown). Furthermore, we could show that candidates, for which we could purify MBP- or GST-fusions of sufficient quality, could bind overexpressed LUBAC subunits HOIP and HOIL-1L (Supplementary Figure 4B). Next, we utilised the recombinant tandem of 3 NEMO UBAN domains (superUBAN), to pull-down linear polyUb-modified substrates. Upon LUBAC overexpression, the amount of HMW HA-tagged TRAF6 pulled down with the superUBAN was significantly increased, while the HMW species of the other HA-tagged substrates only bound to superUBAN when LUBAC was co-expressed (Figure 5A). Binding to HMW Ub species of putative substrates was specific, since it was abolished when NEMO Ub-binding deficient mutant F305A (superUBAN F305A) was used (Figure 5A). Moreover, we could observe linear polyUb HMW species above all the HA- and MYC-tagged putative LUBAC substrates when we immunoprecipitated them under denaturing conditions from the samples with ectopically expressed LUBAC complex (Figure 5B). Furthermore, we used 1F11/3F5/Y102L antibody[5], to immunoprecipitate linear polyUb-modified proteins under denaturing conditions from the samples containing overexpressed active LUBAC. We could detect HMW species above substrates with anti-HA antibody, strongly indicating linear polyubiquitination of putative LUBAC substrates (Figure 5C). Moreover, we performed an *in vitro* ubiquitination assay with recombinant active LUBAC and recombinant candidates. TRAF6 is an adaptor protein and E3 ligase which generates K63-linked polyUb chains and ubiquitinates itself as well as several proteins including NEMO and AKT1[43,44]. Moreover, deacetylase HDAC6 has also been suggested to possess intrinsic E3 ligase activity[45]. Thus, an additional control was applied for TRAF6 and HDAC6. We could show that SEPT2, HDAC6, VDAC1 and TRAF6 are polyubiquitinated by LUBAC *in vitro* (Supplementary Figure 4C). Also, the observed increase of wild-type TRAF6 ubiquitination in the presence of LUBAC was decreased when samples were additionally treated with active OTULIN (Supplementary Figure 4D), further confirming its linear ubiquitination.

We analysed the TRAF6 sample (from Figure 5B) by MS and could identify the characteristic linear polyUb peptide GGMQIFVK (Supplementary Figure 4E and Supplementary Table 1). As the final proof, we immunoprecipitated linear polyUb-modified proteins under denaturing conditions from the samples containing ectopic LUBAC complex and detected HMW species of several endogenous putative substrates (Supplementary Figure 4F).

**The Functional Significance of TRAF6 Linear Polyubiquitination**. Despite relatively low enrichment of TRAF6 in MS screen, TRAF6 proved to be very potent MS candidate during the evaluation of putative linear polyUb-modified substrates. Therefore, we hypothesised that TNFα (originally used in our MS experiment) might not be the optimal physiological stimulus for the linear polyubiquitination of TRAF6. Since TRAF6 is involved in IL-1β-dependent NFκB signalling[46], we compared the ability of IL-1β and TNFα to induce linear polyubiquitination of TRAF6. Our data show that IL-1β-dependent linear polyubiquitination of TRAF6 is stronger than the one induced by TNFα (Figure 6A). When we additionally silenced HOIP expression by siRNA approach, IL-1β failed to induce linear polyubiquitination of TRAF6 (Supplementary Figure 5A), confirming that LUBAC modifies TRAF6 with linear polyUb chains. Next, we tested if E3 ligase activity of TRAF6 is a prerequisite for its linear polyubiquitination. We could demonstrate that recombinant catalytically inactive TRAF6 C70A mutant is also modified by LUBAC (Figure 6B). Thus, TRAF6 E3 ligase activity is not required for its subsequent linear polyubiquitination, with LUBAC directly modifying TRAF6 by linear polyUb chains, and not requiring priming with K63-linked chains. By MS, we identified three K-residues of TRAF6 ubiquitinated upon LUBAC overexpression: one within coiled-coil motif that was previously reported (K339[31]) and two novel sites within MATH domain (K497 and K518) (Figure 6C, Supplementary Figure 5B and Supplementary Table 1). Interestingly, K339 and K497 are conserved among species, suggesting their physiological significance. When we tested the ability of recombinant TRAF6 C70A and TRAF6 C70A K339/K497/K518R mutants to be modified by LUBAC *in vitro* (Supplementary Figures 5C-5D), triple K339/K497/K518R TRAF6 mutant failed to be ubiquitinated. Similarly, immunoprecipitated TRAF6 K339/K497/K518R mutant could not be efficiently modified by linear polyUb chains upon IL-1β stimulation (Figure 6D), confirming that the identified residues of TRAF6 are the major targets for LUBAC-mediated polyubiquitination. To further study the importance of linear polyubiquitination of TRAF6 in NFκB pathway, we tested phosphorylation and degradation of IκBα (Supplementary Figure 5E), as well as NFκB transcriptional activity (Figure 6E) in TRAF6$^{-/-}$ MEFs reconstituted with various TRAF6 mutants (Supplementary Figure 5F). As expected,

degradation of IκBα in IL-1β-stimulated TRAF6$^{-/-}$ MEFs reconstituted with either empty vector or TRAF6 C70A was abolished, confirming the crucial role of TRAF6 E3 ligase activity in IL-1β-induced NFκB signalling. Reconstitution of TRAF6$^{-/-}$ MEFs with wild-type TRAF6 restored phosphorylation and degradation of IκBα. Interestingly, TRAF6$^{-/-}$ MEFs reconstituted with TRAF6 K339/K497/K518R mutant could activate the NFκB pathway but could not sustain the activating effect on the pathway. Expression of TRAF6 K32-518R mutant also resulted with the impaired IκBα degradation. The effect of both TRAF6 K-deficient mutants on NFκB transcriptional activity is even more striking, as both TRAF6 K339/K497/K518R and TRAF6 K32-518R inhibit IL-1β-induced NFκB activity. Therefore, both TRAF6 E3 ligase activity and its linear polyubiquitination are essential for proper IL-1β-induced NFκB signalling.

**DISCUSSION**

Knowledge about the recently discovered linear polyUb modification is limited by a lack of adequate methods that permit identification of linear polyUb-modified proteins. Here, we introduce a K-less internally tagged Ub approach combined with MS, to identify novel linear polyUb targets in a simple and robust manner.

Ub is rather small, highly conserved eukaryotic protein with the majority of its surfaces being required for the interaction with Ub machinery (E1, E2, E3, DUB) or UBD-containing proteins. Nevertheless, our choice of the insertion point and insertion tag within Ub fully maintains the structural and functional integrity of Ub both *in vitro* and *in vivo*, thereby representing the first report of the functional internally tagged Ub.

In order to test our method, we shortly stimulated cells with TNFα[5] and performed Strep-Tactin® PD under denaturing conditions. We identified several novel linear polyUb-modified proteins, significantly expanding the number of known linear polyUb targets. Since proteins found near MS background (i.e. TRAF6 and VDAC1) were also shown to be modified by linear polyUb chains, INT-Ub.7KR approach has proven to be a potent and sensitive method for the discovery of linear polyUb-modified proteins.

The major limitations of our approach are related to MS detection sensitivity, as well as protein abundance of linear polyUb targets in tested cell lines. Usually, only a small pool of the protein is modified by linear polyUb chains. If the protein is expressed at low levels, MS signals from very low abundant modified proteins will be close to noise levels and will not have high SILAC ratios.

The E3 ligase complex LUBAC is so far the only known enzyme known to generate linear

polyUb chains. Nevertheless, INT-Ub.7KR approach enables identification of both LUBAC-dependent and even LUBAC-independent linear ubiquitination, since it does not rely on using LUBAC during the screen. By combining INT-Ub.7KR with other stimuli (such as DNA damage-inducing compounds, heat shock, various pathogen infections) it is possible to identify stimulation-specific linear polyubiquitination substrates (and in that way, novel processes regulated by linear polyubiquitination), which can be both LUBAC-dependent, and potentially LUBAC-independent.

Since INT-Ub.7KR maintains Ub fold and does not lead to cellular toxicity when expressed at low levels, the generation of knock-in animal models would enable the study of linear polyubiquitination during development and its cellular roles in both normal and pathological conditions.

Moreover, identification of novel linear polyUb targets, beyond a handful of proteins identified since 2006[7,18,22-24], will hopefully enable the development of targeted therapy for diseases caused by impaired linear polyubiquitination.

Overall, INT-Ub.7KR approach will significantly contribute to the understanding of until now largely underestimated spectrum of linear polyubiquitination, expanding the current view of its cellular roles.

## ACCESSION CODES

The MS proteomics data have been deposited to the ProteomeXchange Consortium (http://proteomecentral.proteomexchange.org) via the PRIDE partner repository[47] with the dataset identifier PXD005878.

## DATA AVAILABILITY STATEMENT

The authors declare that the data supporting the findings of this study are available within the paper and its supplementary files.

## ACKNOWLEDGMENTS

We thank Minoru Asada (Nippon Medical School), Rohan T. Baker (Clinical Genomics), Anja Bremm (Goethe University School of Medicine), Christian Behrends (Goethe University School of Medicine), Jue Chen (Rockefeller University), Kyung-Hee Chun (Yonsei University College of Medicine), Ivan Dikic (Goethe University School of Medicine), Hui Jiang (National Institute of Biological Sciences), Jae U. Jung (University of Southern California), Masahiko Kobayashi (Kanazawa University), Carl White (Rosalind Franklin

University of Medicine and Science) and Alfred Wittinghofer (Max Planck Institute of Molecular Physiology) for providing reagents and M. Akutsu, A. Carpy, J. Lopez-Mosqueda, M. Olma and S. Wahl for initial help with the project. We thank S. Schaubeck for excellent technical assistance. We are especially grateful to Jun-Ichiro Inoue (University of Tokyo) for providing us with TRAF6$^{-/-}$ MEFs and J. W. Bowman for providing us with the detailed LUBAC purification protocol. We thank A. Bremm, J. Lopez-Mosqueda and B. Srinivasan for discussions, comments and reading of the manuscript. We would also like to thank Reviewer 1 for their comments, which helped us to substantially improve the manuscript. K.K. was supported by the UPStream grant (EU, FP7, ITN project 290257).

## AUTHOR CONTRIBUTIONS

K.H. and K.K. developed the concept and designed the experiments. K.H. developed the INT-Ub tool, prepared the constructs and performed initial validation experiments. K.K. optimized the method, carried out all the cell biology and biochemical experiments, prepared all the inducible cell lines and samples for MS experiments and analysed the results, including MS data. B.M., C.T. and M.F.W. performed and analysed MS data. B.S., I.P. and S.K. performed and analysed CD and NMR experiments. K.H. and K.K. wrote the manuscript, with the contribution of all the authors.

## COMPETING FINANCIAL INTERESTS STATEMENT

The authors declare no competing financial interests.

## REFERENCES

1 Varshavsky, A. Regulated protein degradation. *Trends in biochemical sciences* **30**, 283-286, doi:10.1016/j.tibs.2005.04.005 (2005).

2 Hershko, A. & Ciechanover, A. The ubiquitin system. *Annual review of biochemistry* **67**, 425-479, doi:10.1146/annurev.biochem.67.1.425 (1998).

3 Kulathu, Y. & Komander, D. Atypical ubiquitylation - the unexplored world of polyubiquitin beyond Lys48 and Lys63 linkages. *Nature reviews. Molecular cell biology* **13**, 508-523, doi:10.1038/nrm3394 (2012).

4 Kirisako, T. *et al.* A ubiquitin ligase complex assembles linear polyubiquitin chains. *The EMBO journal* **25**, 4877-4887, doi:10.1038/sj.emboj.7601360 (2006).

5 Matsumoto, M. L. *et al.* Engineering and structural characterization of a linear polyubiquitin-specific antibody. *Journal of molecular biology* **418**, 134-144, doi:10.1016/j.jmb.2011.12.053 (2012).

6 Phu, L. *et al.* Improved quantitative mass spectrometry methods for characterizing complex ubiquitin signals. *Molecular & cellular proteomics : MCP* **10**, M110 003756, doi:10.1074/mcp.M110.003756 (2011).

7 Tokunaga, F. *et al.* Involvement of linear polyubiquitylation of NEMO in NF-kappaB activation. *Nature cell biology* **11**, 123-132, doi:10.1038/ncb1821 (2009).

8 Asaoka, T. *et al.* Linear ubiquitination by LUBEL has a role in Drosophila heat stress response. *EMBO reports* **17**, 1624-1640, doi:10.15252/embr.201642378 (2016).
9 Damgaard, R. B. *et al.* The ubiquitin ligase XIAP recruits LUBAC for NOD2 signaling in inflammation and innate immunity. *Molecular cell* **46**, 746-758, doi:10.1016/j.molcel.2012.04.014 (2012).
10 Shimizu, Y., Taraborrelli, L. & Walczak, H. Linear ubiquitination in immunity. *Immunological reviews* **266**, 190-207, doi:10.1111/imr.12309 (2015).
11 Tokunaga, F. Linear ubiquitination-mediated NF-kappaB regulation and its related disorders. *Journal of biochemistry* **154**, 313-323, doi:10.1093/jb/mvt079 (2013).
12 Okamura, K. *et al.* Survival of mature T cells depends on signaling through HOIP. *Scientific reports* **6**, 36135, doi:10.1038/srep36135 (2016).
13 Teh, C. E. *et al.* Linear ubiquitin chain assembly complex coordinates late thymic T-cell differentiation and regulatory T-cell homeostasis. *Nature communications* **7**, 13353, doi:10.1038/ncomms13353 (2016).
14 Sasaki, Y. *et al.* Defective immune responses in mice lacking LUBAC-mediated linear ubiquitination in B cells. *The EMBO journal* **32**, 2463-2476, doi:10.1038/emboj.2013.184 (2013).
15 Smit, J. J. *et al.* The E3 ligase HOIP specifies linear ubiquitin chain assembly through its RING-IBR-RING domain and the unique LDD extension. *The EMBO journal* **31**, 3833-3844, doi:10.1038/emboj.2012.217 (2012).
16 Stieglitz, B. *et al.* Structural basis for ligase-specific conjugation of linear ubiquitin chains by HOIP. *Nature* **503**, 422-426, doi:10.1038/nature12638 (2013).
17 Ikeda, F. *et al.* SHARPIN forms a linear ubiquitin ligase complex regulating NF-kappaB activity and apoptosis. *Nature* **471**, 637-641, doi:10.1038/nature09814 (2011).
18 Gerlach, B. *et al.* Linear ubiquitination prevents inflammation and regulates immune signalling. *Nature* **471**, 591-596, doi:10.1038/nature09816 (2011).
19 Tokunaga, F. *et al.* SHARPIN is a component of the NF-kappaB-activating linear ubiquitin chain assembly complex. *Nature* **471**, 633-636, doi:10.1038/nature09815 (2011).
20 Keusekotten, K. *et al.* OTULIN antagonizes LUBAC signaling by specifically hydrolyzing Met1-linked polyubiquitin. *Cell* **153**, 1312-1326, doi:10.1016/j.cell.2013.05.014 (2013).
21 Rivkin, E. *et al.* The linear ubiquitin-specific deubiquitinase gumby regulates angiogenesis. *Nature* **498**, 318-324, doi:10.1038/nature12296 (2013).
22 Fiil, B. K. *et al.* OTULIN restricts Met1-linked ubiquitination to control innate immune signaling. *Molecular cell* **50**, 818-830, doi:10.1016/j.molcel.2013.06.004 (2013).
23 Rodgers, M. A. *et al.* The linear ubiquitin assembly complex (LUBAC) is essential for NLRP3 inflammasome activation. *The Journal of experimental medicine* **211**, 1333-1347, doi:10.1084/jem.20132486 (2014).
24 Satpathy, S. *et al.* Systems-wide analysis of BCR signalosomes and downstream phosphorylation and ubiquitylation. *Molecular systems biology* **11**, 810, doi:10.15252/msb.20145880 (2015).
25 Emmerich, C. H. *et al.* Activation of the canonical IKK complex by K63/M1-linked hybrid ubiquitin chains. *Proceedings of the National Academy of Sciences of the United States of America* **110**, 15247-15252, doi:10.1073/pnas.1314715110 (2013).
26 Smahi, A. *et al.* Genomic rearrangement in NEMO impairs NF-kappaB activation and is a cause of incontinentia pigmenti. The International Incontinentia Pigmenti (IP) Consortium. *Nature* **405**, 466-472, doi:10.1038/35013114 (2000).

27 Doffinger, R. *et al.* X-linked anhidrotic ectodermal dysplasia with immunodeficiency is caused by impaired NF-kappaB signaling. *Nature genetics* **27**, 277-285, doi:10.1038/85837 (2001).
28 Filipe-Santos, O. *et al.* X-linked susceptibility to mycobacteria is caused by mutations in NEMO impairing CD40-dependent IL-12 production. *The Journal of experimental medicine* **203**, 1745-1759, doi:10.1084/jem.20060085 (2006).
29 Xu, G., Paige, J. S. & Jaffrey, S. R. Global analysis of lysine ubiquitination by ubiquitin remnant immunoaffinity profiling. *Nature biotechnology* **28**, 868-873, doi:10.1038/nbt.1654 (2010).
30 Wagner, S. A. *et al.* A proteome-wide, quantitative survey of in vivo ubiquitylation sites reveals widespread regulatory roles. *Mol Cell Proteomics* **10**, M111 013284, doi:10.1074/mcp.M111.013284 (2011).
31 Kim, W. *et al.* Systematic and quantitative assessment of the ubiquitin-modified proteome. *Molecular cell* **44**, 325-340, doi:10.1016/j.molcel.2011.08.025 (2011).
32 Danielsen, J. M. *et al.* Mass spectrometric analysis of lysine ubiquitylation reveals promiscuity at site level. *Molecular & cellular proteomics : MCP* **10**, M110 003590, doi:10.1074/mcp.M110.003590 (2011).
33 Meierhofer, D., Wang, X., Huang, L. & Kaiser, P. Quantitative analysis of global ubiquitination in HeLa cells by mass spectrometry. *Journal of proteome research* **7**, 4566-4576, doi:10.1021/pr800468j (2008).
34 Peng, J. *et al.* A proteomics approach to understanding protein ubiquitination. *Nature biotechnology* **21**, 921-926, doi:10.1038/nbt849 (2003).
35 Rahighi, S. *et al.* Specific recognition of linear ubiquitin chains by NEMO is important for NF-kappaB activation. *Cell* **136**, 1098-1109, doi:10.1016/j.cell.2009.03.007 (2009).
36 Baker, R. T. *et al.* Using deubiquitylating enzymes as research tools. *Methods in enzymology* **398**, 540-554, doi:10.1016/S0076-6879(05)98044-0 (2005).
37 Povlsen, L. K. *et al.* Systems-wide analysis of ubiquitylation dynamics reveals a key role for PAF15 ubiquitylation in DNA-damage bypass. *Nature cell biology* **14**, 1089-1098, doi:10.1038/ncb2579 (2012).
38 Haas, T. L. *et al.* Recruitment of the linear ubiquitin chain assembly complex stabilizes the TNF-R1 signaling complex and is required for TNF-mediated gene induction. *Molecular cell* **36**, 831-844, doi:10.1016/j.molcel.2009.10.013 (2009).
39 Takiuchi, T. *et al.* Suppression of LUBAC-mediated linear ubiquitination by a specific interaction between LUBAC and the deubiquitinases CYLD and OTULIN. *Genes to cells : devoted to molecular & cellular mechanisms* **19**, 254-272, doi:10.1111/gtc.12128 (2014).
40 Lewis, M. J. *et al.* UBE2L3 polymorphism amplifies NF-kappaB activation and promotes plasma cell development, linking linear ubiquitination to multiple autoimmune diseases. *American journal of human genetics* **96**, 221-234, doi:10.1016/j.ajhg.2014.12.024 (2015).
41 Muller-Rischart, A. K. *et al.* The E3 ligase parkin maintains mitochondrial integrity by increasing linear ubiquitination of NEMO. *Molecular cell* **49**, 908-921, doi:10.1016/j.molcel.2013.01.036 (2013).
42 Khan, M., Syed, G. H., Kim, S. J. & Siddiqui, A. Hepatitis B Virus-Induced Parkin-Dependent Recruitment of Linear Ubiquitin Assembly Complex (LUBAC) to Mitochondria and Attenuation of Innate Immunity. *PLoS Pathog* **12**, e1005693, doi:10.1371/journal.ppat.1005693 (2016).
43 Lamothe, B. *et al.* Site-specific Lys-63-linked tumor necrosis factor receptor-associated factor 6 auto-ubiquitination is a critical determinant of I kappa B kinase

activation. *The Journal of biological chemistry* **282**, 4102-4112, doi:10.1074/jbc.M609503200 (2007).
44 Yang, W. L. *et al.* The E3 ligase TRAF6 regulates Akt ubiquitination and activation. *Science* **325**, 1134-1138, doi:10.1126/science.1175065 (2009).
45 Zhang, M. *et al.* HDAC6 deacetylates and ubiquitinates MSH2 to maintain proper levels of MutSalpha. *Molecular cell* **55**, 31-46, doi:10.1016/j.molcel.2014.04.028 (2014).
46 Deng, L. *et al.* Activation of the IkappaB kinase complex by TRAF6 requires a dimeric ubiquitin-conjugating enzyme complex and a unique polyubiquitin chain. *Cell* **103**, 351-361 (2000).
47 Vizcaino, J. A. *et al.* 2016 update of the PRIDE database and its related tools. *Nucleic Acids Res* **44**, D447-456, doi:10.1093/nar/gkv1145 (2016).

**FIGURE LEGENDS**

**Figure 1. The design and *in vitro* validation of INT-Ub.** (**A**) Ub molecule with an insertion point of STREP-tag® II (black) and the following color-coded residues: K (red), M (orange), G76 (blue) and I44 (yellow). This Figure was generated with PyMOL software by modifying the 1UBQ.pdb file. **(B)** A comparison of 1D 1H NMR spectra of INT-Ub with unmodified Ub. (**C**) Testing the ability of INT-Ub to form various polyUb chains in *in vitro* ubiquitination assays. INT-Ub.ΔGG served as a negative control. (**D**) Examination of interaction between INT-diUb and UBAN by pull-down assay. (**E**) *In vitro* deubiquitination assay with recombinant INT-diUb and DUBs USP2-cc or (**F**) OTULIN. Blot images for Figures 1C-1F were cropped to improve the conciseness of the presentation (full blots are available in Supplementary Figure 6).

**Figure 2. *In vivo* validation of INT-Ub.** (**A**) Comparison of INT-Ub (lane 1), INT-Ub.7KR (lane 2) and INT-Ub.ΔGG (lane 3) abilities to conjugate into polyUb chains *in vivo*. (**B**) MS identification of GG-K48-INT-Ub and GG-K63-INT-Ub peptides in INT-Ub IP sample. MS/MS spectra of the GG-K48-INT-Ub (top panel) and GG-K63-INT-Ub (lower panel) peptides are shown. (**C**) Comparative pull-down assay to test the ability of INT-Ub and INT-Ub.ΔGG to enrich polyubiquitinated substrates. Mono- and double monoubiquitinated forms of PAF15 were present in INT-Ub PD, but not in INT-Ub.ΔGG PD. (**D**) Effect of INT-Ub variants on p65 nuclear translocation upon TNFα (20 ng/ml, 30 min) stimulation. Analysis of p65 translocation into nucleus by measuring its abundance in cytoplasmic and nuclear cellular fractions in T-REx HEK293T cell lines expressing various Ub variants. PCNA and GAPDH were used as nuclear and cytoplasmic markers, respectively. (**E**) Quantification of (**D**) by ImageJ software. Results are shown as means and s.e.m. (n=3). n.s=no statistically significant difference ($p>0.05$), determined by the two tailed Student's t-test. (**F**) Effect of INT-Ub variants on NFκB transcriptional activity upon TNFα (20 ng/ml, 10 h) stimulation. Measurement of NFκB transcriptional activity by luciferase assay in T-REx HEK293T cell lines expressing various Ub variants. Results are shown as means and s.e.m. (n=3). *$p<0.05$, n.s=no statistically significant difference ($p>0.05$), determined by the two tailed Student's t-test. Blot images for Figures 2A, 2C and 2D were cropped to improve the conciseness of the presentation (full blots are available in Supplementary Figure 6).

**Figure 3**. **The use of lysine-less INT-Ub for the identification of novel LUBAC substrates.** Effect of OTULIN silencing by siRNA (**A**), OTULIN C129A mutant overexpression (**B**), LUBAC components overexpression (**C**), and TNFα treatment (**D**) on the abundance of HMW Ub species in INT-Ub.7KR Strep-Tactin® PD, compared to control

conditions. (**E**) As in (**B**), but sample was immunoblotted with anti-STREP antibody. (**F**) As in (**A**), but sample was immunoblotted with anti-Lub9 antibody to detect linear polyubiquitination. Blot images for Figure 3 were cropped to improve the conciseness of the presentation (full blots are available in Supplementary Figure 7).

**Figure 4**. **Mass spectrometry-based identification of novel linear polyUb-modified substrates**. (**A**) Schematic representation of the SILAC-based MS proteomic approach for the identification of linear polyUb-modified substrates upon 10 min of TNFα stimulation. (**B**) Kyoto Encyclopaedia of Genes and Genomes (KEGG) pathway analysis and (**C**) Gene Ontology (GO) annotation enrichment analysis of proteins upregulated in MS analysis performed in (**A**). The bar plot shows significantly over-represented KEGG and GO molecular function (GOMF) terms, respectively. The enriched KEGG pathways and GOMF terms were identified according to their enrichment (Fisher´s exact test, $p<0.01$). (**D**) Scatter plots shown as a function of protein intensity and SILAC ratios (left: L/H, middle: L/M and right: M/H) for MS data in (**A**) and Supplementary Table 2. SILAC ratios of log2>1 are marked in red. Putative LUBAC substrates selected for the final validation are indicated in the plots. The number of quantified protein pairs are marked in left upper part of each plot.

**Figure 5. Validation of novel linear polyUb-modified substrates. (A)** Pull-down assay between either GST, GST NEMO UBANx3 or GST NEMO UBANx3 F305A mutant and HMW species of HA-tagged putative linear polyUb-modified substrates, which were transiently co-overexpressed with LUBAC components in HEK293T cells. (**B**) Analysis of the presence of HMW linear polyUb-modified species of either HA- or MYC-tagged putative substrates by denaturing IP. Putative substrates were transiently co-overexpressed with HOIP and HOIL-1L in HEK293T cells. (**C**) Verification of the presence of HMW species of HA-tagged putative substrates by linear Ub IP. HA-tagged putative substrates were transiently co-overexpressed with active LUBAC components in HEK293T cells. For experiments **(A-C)** HEK293T cells transfected only with tagged putative substrates and empty vector were used. Blot images for Figure 5 were cropped to improve the conciseness of the presentation (full blots are available in Supplementary Figures 8-10).

**Figure 6. TRAF6 is a novel LUBAC substrate in NFκB signalling. (A)** Denaturing IP comparing IL-1β and TNFα for their efficiency to induce linear polyubiquitination of TRAF6 in TRAF6$^{-/-}$ MEFs reconstituted with HA-TRAF6. **(B)** *In vitro* ubiquitination assay with recombinant HOIP and HOIL-1L and a catalytically inactive TRAF6 C70A mutant. **(C)** Schematic representation of mouse TRAF6. Ubiquitinated residues identified by MS are shown as yellow stars. Below: alignment of the TRAF6 region surrounding the modified K

residues in selected vertebrates. (**D**) Denaturing IP from TRAF6$^{-/-}$ MEFs reconstituted with either HA-TRAF6 or HA-TRAF6 K339,497,518R to compare their linear polyubiquitination upon IL-1β (10 ng/ml, 5 min) *in vivo*. (**E**) Effect of TRAF6 variants on NFκB transcriptional activity. TRAF6$^{-/-}$ MEFs expressing various TRAF6 variants were starved for 16 h and stimulated with IL-1β (10 ng/ml) for 10 h and subjected to a luciferase assay. Results are shown as means and s.e.m. (n=4). **p<0.01, *p<0.05, determined by the two tailed Student's t-test. Blot images for Figure 6A, 6B and 6D were cropped to improve the conciseness of the presentation (full blots are available in Supplementary Figure 11).

## ONLINE METHODS

**Cloning and Antibodies.** The lists of generated and received plasmids and antibodies are available respectively in Supplementary Tables 3 and 4.

**Cell Lines.** Cell lines HEK293T, T-REx HEK293T (T-REx™-293) and T-REx HeLa (T-REx™-HeLa) were purchased respectively from ATCC and Invitrogen. Early passages were propagated, frozen at -150°C and aliquots were used for a limited number of passages. TRAF6$^{-/-}$ MEFs were obtained from Dr Jun-Ichiro Inoue. All cells were regularly checked for *Mycoplasma* infection using Venor®GeM Classic from Minerva Biolabs GmbH (Ltd.).

**Purification of MBP-, GST-, HIS- and STREP-tag® Protein Fusions.** Various MBP and GST fusions were purified as shown previously[48]. STREP-tag® INT-Ub proteins were purified according to Qiagen's protocol. Briefly, a bacterial pellet was thawed and resuspended in buffer NP (50 mM $NaH_2PO_4$ and 300 mM NaCl; pH 8.0) together with 1 mg/ml lysozyme and 3 U/ml benzonase. After incubation on ice (30 min) lysate was sonicated, centrifuged (10000 g, 20 min, 4°C) and supernatant incubated with Strep-Tactin® Sepharose® (IBA, 1 h, 4°C with rotation). INT-Ub proteins bound to Strep-Tactin® Sepharose® were washed with buffer NP and eluted with buffer NPD (50 mM $NaH_2PO_4$, 300 mM NaCl and 2.5 mM desthiobiotin; pH 8.0). Proteins for structural characterisation by CD-spectroscopy were further purified by size exclusion chromatography using a Superdex S75 column (GE Healthcare) in 50 mM HEPES (pH 7.4) and 150 mM NaCl. Fractions of highly pure Ub variants were identified by SDS-PAGE and subsequently concentrated using Vivaspin® Protein Concentrators (GE Healthcare). The proteins GST-UBE2S-UBD, GST-AMSH, GST-NIeL, GST-CBL RF, MBP-HOIP RBR-C and 6xHIS-USP2-cc were purified as previously described[36,49-53]. After purification, UBE2S-UBD, OTULIN and NIeL were then respectively cleaved with PreScission™ (GE Healthcare) and TEV (Invitrogen) proteases to remove GST moiety. HOIL-1L-6xHIS, HOIP-6xHIS, 6xHIS-SEPT2, 6xHIS-VDAC1 and 6xHIS-TRAF6, in addition to its mutants, were purified as previously described[23].

**GST and MBP Pull-down Assays.** HEK293T cells were transiently transfected with indicated plasmids using GeneJuice® (Merck Millipore). Twenty-four to forty-eight hours post transfection cells were lysed in a lysis buffer (50 mM HEPES, pH 7.5; 150 mM NaCl, 1 mM EDTA, 1 mM EGTA, 10 mM $ZnCl_2$, 10% glycerol, 1 % Triton X-100, 25 mM NaF, 2 mM NEM, 1 mM PMSF and complete protease and phosphatase inhibitors (Roche)). Cell lysates were incubated with either GST- or MBP-fused proteins bound respectively to glutathione sepharose beads or amylose resin. After overnight incubation, samples were washed three times in a lysis buffer and eluted from resins by incubation in a 1x LDS buffer

supplemented with β-mercaptoethanol (10 min, 70°C). To test direct interactions, either eluted or cleaved recombinant GST- or MBP-tagged proteins were incubated respectively with MBP- or GST-fused proteins bound to amylose resin or glutathione sepharose resin in an incubation buffer (20 mM Tris-HCl, pH 8.4; 150 mM NaCl, 2.5 mM $CaCl_2$, 10 % glycerol, 1 % Triton X-100 and 1 mM DTT) at 4°C. After 4 h incubation, samples were washed three times in an incubation buffer and eluted from resins by incubation in a 1x LDS buffer supplemented with β-mercaptoethanol (10 min, 70°C).

**SuperUBAN Pull-down Assays.** The assay was modified from[23]. Briefly, GST-tagged superUBAN (UBANx3) and superUBAN F305A (UBANx3 F305A) were purified as described above. HEK293T cells were transfected with indicated constructs using GeneJuice®. Twenty-four hours post transfection cells were lysed in a pull-down buffer (50 mM Tris-HCl, pH 7.4; 150 mM NaCl, 1 % NP-40, 0.5 % DOC, 10 mM NEM and complete protease and phosphatase inhibitors (Roche)), sonicated for 20 s at 10 % and treated with benzonase. Protein concentrations were measured and adjusted, and lysates were then precleared with GST protein bound to glutathione sepharose resins (1 h, 4°C with rotation). Cleared lysates were then incubated with GST, GST UBANx3 or GST UBANx3 F305A bound to glutathione sepharose (overnight, 4°C with rotation). Samples were washed three times in a pull-down buffer and eluted from resins by incubation in a 1x LDS buffer supplemented with β-mercaptoethanol (10 min, 70°C). In cases where samples were prepared for MS analysis, they were additionally washed twice in $ddH_2O$ supplemented with 2 mM NEM before elution.

***In vitro* Ubiquitination Reaction**. The enzymes 6xHIS-E1, UBCH5a, UBCH5c, 6xHIS-UBC13/UEV1 (all Boston Biochem) and UBCH7 (Merck Millipore) were purchased. MBP-HDAC6 was purified as described above followed by overnight cleavage with factor Xa at room temperature. Reactions contained 200 ng E1, 400 ng UBCH5c, 1 μg purified 6xHIS-HOIL-1L/HOIP, 1 μg 6xHIS-SEPT2, 1 μg 6xHIS-VDAC1, 2 μg MBP-HDAC6, 1 μg 6xHIS-TRAF6 variant, 10 μg Ub, 2 mM ATP, 20 mM Tris-HCl (pH 7.5), 5 mM $MgCl_2$ and 2 mM DTT. The assay was performed at 37°C for 3 h and stopped by adding a 1x LDS buffer supplemented with β-mercaptoethanol. Reactions with UBE2S-UBD and AMSH, NIeL, CBL RF, HOIP RBR-C and USP2-cc were performed as previously described[36,49-52]. All the other reactions were performed by incubating E1 (150 ng), E2 (300 ng), E3 (2 μg), Ub or INT-Ub variants (1 μg) with or without 2 mM ATP in *in vitro* ubiquitination buffer (50 mM Tris-HCl,

pH 7.5; 5 mM $MgCl_2$, 2 mM DTT) for 1 h at 37°C. To stop reactions, a 1x LDS buffer supplemented with β-mercaptoethanol was added.

**Deubiquitinase Assays.** Reactions with USP2-cc and OTULIN were performed as described previously[36,54].

**CD Measurements**. Far-UV CD spectra were recorded on a Jasco J-815 spectropolarimeter fitted with a cell holder thermostatted by a CDF-426S Peltier unit. All CD measurements were made in 50 mM sodium phosphate buffer (pH 7.4) at 20°C using fused silica cuvettes with 1 mm path lengths (Hellma, Jena, Germany). The spectra were recorded with 0.2 nm resolution and baseline corrected by subtraction of the appropriate buffer spectrum. CD intensities are presented as the CD absorption coefficient calculated on a mean residue weight basis ($\Delta\varepsilon_{MRW}$)[55]. In order to visualise the overlapping shape of all four Ub variants, the spectra of INT-Ub.7KR were multiplied by 1.3, which accounts for a slight overestimation of the protein concentration.

**NMR Spectroscopy.** All measurements were performed at 293 K in 20 mM HEPES (pH 7.4), 50 mM NaCl, 10% $D_2O$ on a Bruker AV600 spectrometer.

**Preparation of Inducible Cell Lines for MS Analysis.** Stable inducible T-Rex HEK293T cell lines were metabolically labelled by SILAC (*stable isotope labelling by amino acids in cell culture*) approach. The stable T-REx HEK293T cell lines INT-Ub, INT-Ub.7KR and INT-Ub.ΔGG were cultured in media containing heavy L-Arg (R10)/L-Lys (K8) ("heavy"), medium L-Arg (R6)/L-Lys (K4) ("medium") and light L-Arg (R0)/L-Lys (K0) ("light"), as indicated in Figure 4A and Supplementary Figure 4A. When kept in medium containing zeocin (300 μg/ml) and blasticidin (10 μg/ml), INT-Ub expression was silenced.

**Strep-Tactin® Pull-down.** A Strep-Tactin® Pull-down (PD) was performed as follows: stable T-REx HEK293T cell lines were either transfected and/or treated as indicated in the text and expression of various INT-Ub mutants induced by doxycycline treatment (1 μg/ml; 24 h). Cells were lysed in either a denaturing buffer (20 mM Tris-HCl, pH 7.5; 50 mM NaCl, 1 mM EDTA, 0.5 % NP-40, 0.5 % SDS, 0.5 % sodium deoxycholate, 1 mM DTT, 10 mM NEM and a 1x protease inhibitor cocktail) or a modified denaturing buffer (lacking DOC). Cells harvested in a modified denaturing buffer were additionally sonicated for 35 s at amplitude 40 %. After benzonase treatment, protein concentration was adjusted and samples precleared with Superflow resin (30 min, 4°C). Precleared lysates were incubated with prewashed Strep-Tactin® resins (2 h, 4°C) and then subjected to three washing steps in a denaturing buffer. Finally, proteins were eluted by incubation in a 1x LDS buffer supplemented with β-mercaptoethanol (10 min, 70°C).

**Immunoprecipitation.** HA-IP was performed as Strep-Tactin® PD with the exception that anti-HA agarose conjugate was used. Linear Ub IP was performed as described previously[5]. Additionally, linear Ub IP samples were washed twice with $ddH_2O$ supplemented with 10 mM NEM before elution in a 1x LDS buffer supplemented with β-mercaptoethanol (10 min, 70°C). MYC-IP was performed similar to Strep-Tactin® PD, with the exception that cells were lysed in RIPA buffer (50 mM Tris-HCl, pH 7.; 150 mM NaCl, 1 % NP-40, 0.5 % SDS, 0.5 % sodium deoxycholate, 10 mM NEM and a 1x protease inhibitor cocktail) and lysates were subsequently incubated with 0.25 μg of c-Myc antibody and protein G agarose.

**Immunoblotting**. For all the experiments apart from linear Ub IP, immunoblotting was performed as follows: proteins were separated by SDS-PAGE and transferred to either 0.45 μm or 0.22 μm nitrocellulose membrane by wet transfer (200 mA, 2 h). Membranes were blocked either in 5 % BSA in TBS-T or in 5 % milk in TBS-T and probed with indicated primary antibodies overnight at 4°C or for 1 h at RT. Next, membranes were washed in TBS-T, incubated in an appropriate HRP-conjugated secondary antibody for 1 h at RT and washed three times in TBS-T and then twice in TBS. Western Blotting Luminol reagent (Santa Cruz Biotechnologies) or Lumigen TMA-6 (GE Healthcare) were used for antibody visualisation. To visualise linear polyubiquitin fraction, immunoblotting was performed as described previously[5]. For linear Ub IP, endogenous levels of modified proteins were visualised with Clean-Blot IP Detection Reagent (Thermo Fisher Scientific).

**Preparation of Samples for MS Analysis.** An expression of various INT-Ub variants was induced by doxycycline (1 μg/ml; 24 h) and followed by 16 h starvation in a medium lacking FBS. For preliminary MS, experiment cells were stimulated with TNFα (20 ng/ml, 15 min) and harvested in a denaturing buffer (20 mM Tris-HCl, pH 7.5; 50 mM NaCl, 1 mM EDTA, 0.5 % NP-40, 0.5 % SDS, 0.5% sodium deoxycholate, 1 mM DTT, 10 mM NEM and a 1x protease inhibitor cocktail (Roche)) After benzonase treatment, lysates were precleared with prewashed Superflow resins (30 min, 4°C). Protein concentration was measured and lysates were merged in 1:1:1 ratio, followed by incubation with prewashed Strep-Tactin® resins (2 h, 4°C). Resins were then washed three times in a denaturing buffer and then twice in distilled water. Bound proteins were eluted from the Strep-Tactin® resin by incubation in a 1x LDS buffer supplemented with β-mercaptoethanol (10 min, 70°C). In the case of the additional triplicate MS experiment, the following changes were introduced: cells were stimulated with TNFα for 10 min and then lysed in a modified denaturing buffer (lacking DOC). Precleared lysates were incubated with prewashed Strep-Tactin® XT resins.

**Mass Spectrometric Analysis.** Eluates obtained from Strep-Tactin® resins were resolved by SDS-PAGE, each gel lane was cut into 8-15 slices, alkylated with chloroacetamide and digested with trypsin (overnight, 37°C)[56]. Extracted peptides were desalted using $C_{18}$ StageTips[57]. A preliminary MS screen of linear polyUb-modified substrates was performed on an EASY-nLC™ II (Proxeon Biosystems) System coupled to an Orbitrap Elite (Thermo Fisher Scientific) Mass Spectrometer. Peptides were separated on a 15 cm and 75 μm ID PicoTip fused silica emitter (New Objective) in-house packed with ReproSil-Pur® C18-AQ 3 μm resin (Dr Maisch GmbH (Ltd.)). Peptides were eluted from the column using a segmented gradient of 5-50 % of solvent B (80 % ACN in 0.5 % acetic acid) at a constant flow rate of 200 nL/min over 87 or 127 min. The Mass Spectrometer was operated in positive ion mode and spectra were recorded in a mass range from *m/z* 300 to 2,000 with a resolution of 120,000. The twenty most intense ions were selected for collisional-induced dissociation (CID) fragmentation. For targeted MS inclusion lists containing up to 115 peptide masses of interest (ubiquitinated TRAF6 peptides and Ub peptides including modifications and GGM peptide) were exclusively selected for HCD fragmentation and MS/MS acquisition (R=15,000). Additional MS screening for the identification of novel linear polyUb targets was performed on an EASY-nLC™ 1200 System (Thermo Fisher Scientific) coupled to a Q Exactive™ HF (Thermo Fisher Scientific) Mass Spectrometer. Peptides were separated using a segmented gradient of 5-50 % of solvent B (80 % ACN in 0.5 % formic acid) at a constant flow rate of 200 nL/min over 87 min on a 20 cm and 75 μm ID PicoTip fused silica emitter (New Objective) in-house packed with ReproSil-Pur® C18-AQ 1.9 μm resin (Dr Maisch GmbH (Ltd.)). The Q Exactive™ HF was operated in its positive mode. Full scans were acquired from m/z 300 to 1650 with a resolution of 120,000. The seven most intense ions were fragmented by higher-energy collisional dissociation (HCD) and MS/MS spectra recorded with a resolution of 60,000. Experiments were performed in triplicate. Obtained mass spectra were processed with the MaxQuant[58] software suite (version 1.5.1.0) using the internal search engine Andromeda[59] and searched against either the Uniprot *Homo sapiens* (release 2014_02; 88,692 entries) database and a database containing INT-Ub and INT-Ub.7KR sequences or the *Mus musculus* (release 2014_02; 51402 entries) database. Carbamidomethylation (C) was set as fixed modification and acetylation (Protein N-term), oxidation (M), GlyGly (K, N-term), deamidation (N, Q) were defined as variable modifications. In SILAC measurements, the amino acids K4/R6 and K8/R10 were defined as medium and heavy labels, respectively. Mass tolerance at the MS level was set to 4.5 ppm and to 0.5 Da at the MS/MS level (CID fragmentation), or 20 ppm (HCD fragmentation). The false discovery rate for peptides and

proteins was set to 1 %. An arbitrary cut-off of 2-fold change was used to determine significantly SILAC ratios. A functional enrichment analysis (Fisher´s exact test, $p<0.01$) of Gene Ontology and KEGG terms was performed in Perseus (version 1.5.0.15).

**siRNA Silencing.** The following siRNAs (Eurofins Genomics) were used for knockdown: OTULIN1# GAC UGA AAU UUG AUG GGA A; OTULIN2# CAA AUG AGG CGG AGG AAU A; Hoip GAG GAC GGA GUU GUG AGG AUU UCC A and mock GGG AUA CCU AGA CGU UCU A. Knockdown studies were conducted as previously described[20].

**Subcellular Fractionation.** Cells were washed once with ice-cold PBS, resuspended in 100 µl ice-cold buffer A (10 mM HEPES, pH 7.8; 10 mM KCl, 0.1 mM EDTA, 1 mM DTT, 5 µg/ml aprotinin, 2 µM pepstatin, 10 µg/ml leupeptin, 1 mM PMSF, 5 mM NaF, 1 mM $Na_3VO_4$ and 0.5 % Triton X-100), incubated on ice for 10 min and then centrifuged (2000 rpm, 5 min, 4°C). A supernatant was designated the cytoplasmic fraction. The pellet was then washed twice in ice-cold buffer A and resuspended in a 30 µl buffer C (50 mM HEPES, pH 7.8; 420 mM KCl, 0.1 mM EDTA, 5 mM $MgCl_2$, 10 % glycerol, 1 mM DTT 5 µg/ml aprotinin, 2 µM pepstatin, 10 µg/ml leupeptin, 1 mM PMSF, 5 mM NaF and 1 mM $Na_3VO_4$). After 30 min incubation on ice, the pellet was passed several times through a syringe and centrifuged (13000 rpm, 15 min, 4°C). The supernatant was designated the nuclear fraction.

**Luciferase Assays.** Cells were plated on 6-well plates 24 h before transfection. pNFκB-Luc plasmid and β-Gal plasmid were transfected using either GeneJuice® (T-REx HeLa stable cell lines) or TurboFect (reconstituted $TRAF6^{-/-}$ MEFs). Twenty-four hours post transfection, cells were moved to medium lacking FBS for 16 h and then stimulated with either IL-1β (10 ng/ml) or TNFα (20 ng/ml) for indicated times. Cell lysates were subjected to a luciferase assay according to the manufacturer's protocol (Roche). Internal control was measured by β-Gal activity following the manufacturer's protocol (Roche). All experiments were done in biological triplicates, where each biological triplicate consisted of technical duplicates.

**Retroviral production**. Untagged Ub and INT-Ub variants in pBabe–zeocine and HA-tagged mTRAF6 variants in pBabe–puromycin plasmids together with helper plasmid pHAI were transfected in HEK293T cells by using GeneJuice® (Merck Millipore). Thirty-six hours post transfection, media containing retroviruses were filtered, polybrene (4 mg/ml) was added and target cells (Ub variants into T-REx HEK293T/T-REx HeLa and TRAF6 mutants into $TRAF6^{-/-}$ MEFs) were infected. Forty-eight hours later cells were selected with medium containing either zeocine and blasticidin (Ub variants, 300 µg/ml and 10 µg/ml, respectively)

or puromycin (TRAF6 mutants, 4 μg/ml) and kept in medium containing appropriate antibiotic(s).

**Statistical analysis**. To determine statistical significance in Figures 2E, 2F, 6E and Supplementary Figure 2B, an unpaired, two-tailed Student's *t* test was used. Three independent experimental replicates were performed in Figure 2E. Three independent experimental replicates consisting of three technical replicates were performed in Figures 2F and Supplementary Figure 2B. Four independent experimental replicates consisting of three technical replicates were performed in Figure 6E. For all of the figures, results are shown as means and error bars defined as s.e.m. **p<0.01, *$p$<0.05 were considered as significant, while $p$ >0.05 was considered non-significant. T-values and degrees of freedom for t-tests were as follows: Figure 2E (*t*: between 0.0006743 and 2.054, *df*: 4), 2F (*t*: between 0.2587 and 3.506, *df*: 4), 6E (*t*: between 2.892 and 5.612, *df*: 6) and Supplementary Figure 2B (*t*: 1.818, *df*: 4). For Figure 4B and 4C, where functional enrichment analysis of GO and KEGG terms was performed, Fisher´s exact test was used. p<0.01 was considered as significant. The analysis was performed by using Perseus software platform (version 1.5.0.15).

## METHODS-ONLY REFERENCES


48 Aguileta, M. A. *et al.* The E3 Ubiquitin ligase parkin is recruited to the 26S proteasome via the proteasomal ubiquitin receptor Rpn13. *The Journal of biological chemistry*, doi:10.1074/jbc.M114.614925 (2015).

49 Bremm, A. & Komander, D. Synthesis and analysis of K11-linked ubiquitin chains. *Methods in molecular biology* **832**, 219-228, doi:10.1007/978-1-61779-474-2_15 (2012).

50 Lin, D. Y., Diao, J., Zhou, D. & Chen, J. Biochemical and structural studies of a HECT-like ubiquitin ligase from Escherichia coli O157:H7. *The Journal of biological chemistry* **286**, 441-449, doi:10.1074/jbc.M110.167643 (2011).

51 Umebayashi, K., Stenmark, H. & Yoshimori, T. Ubc4/5 and c-Cbl continue to ubiquitinate EGF receptor after internalization to facilitate polyubiquitination and degradation. *Molecular biology of the cell* **19**, 3454-3462, doi:10.1091/mbc.E07-10-0988 (2008).

52 Stieglitz, B., Morris-Davies, A. C., Koliopoulos, M. G., Christodoulou, E. & Rittinger, K. LUBAC synthesizes linear ubiquitin chains via a thioester intermediate. *EMBO reports* **13**, 840-846, doi:10.1038/embor.2012.105 (2012).

53 Catanzariti, A. M., Soboleva, T. A., Jans, D. A., Board, P. G. & Baker, R. T. An efficient system for high-level expression and easy purification of authentic recombinant proteins. *Protein science : a publication of the Protein Society* **13**, 1331-1339, doi:10.1110/ps.04618904 (2004).

54 Licchesi, J. D. *et al.* An ankyrin-repeat ubiquitin-binding domain determines TRABID's specificity for atypical ubiquitin chains. *Nature structural & molecular biology* **19**, 62-71, doi:10.1038/nsmb.2169 (2012).

55 Martin, S. R. & Schilstra, M. J. Circular dichroism and its application to the study of biomolecules. *Methods in cell biology* **84**, 263-293, doi:10.1016/S0091-679X(07)84010-6 (2008).

56 Shevchenko, A., Tomas, H., Havlis, J., Olsen, J. V. & Mann, M. In-gel digestion for mass spectrometric characterization of proteins and proteomes. *Nature protocols* **1**, 2856-2860, doi:10.1038/nprot.2006.468 (2006).

57 Rappsilber, J., Mann, M. & Ishihama, Y. Protocol for micro-purification, enrichment, pre-fractionation and storage of peptides for proteomics using StageTips. *Nature protocols* **2**, 1896-1906, doi:10.1038/nprot.2007.261 (2007).

58 Cox, J. & Mann, M. MaxQuant enables high peptide identification rates, individualized p.p.b.-range mass accuracies and proteome-wide protein quantification. *Nature biotechnology* **26**, 1367-1372, doi:10.1038/nbt.1511 (2008).

59 Cox, J. *et al.* Andromeda: a peptide search engine integrated into the MaxQuant environment. *Journal of proteome research* **10**, 1794-1805, doi:10.1021/pr101065j (2011).

# Figure 1.

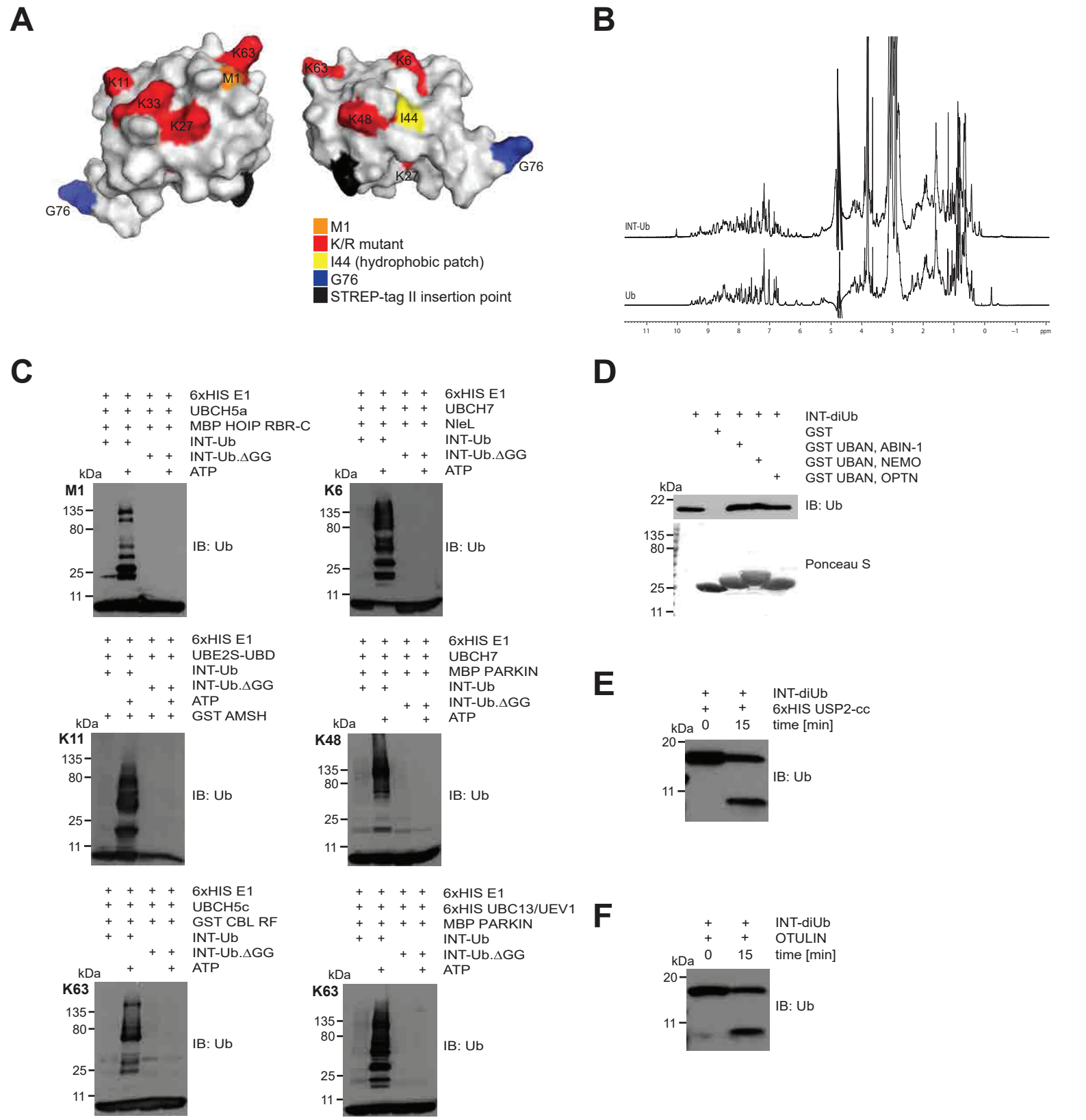
A
K63
K11
M1
K33
K27
G76
K63
K6
K48
I44
K27
G76
M1
K/R mutant
I44 (hydrophobic patch)
G76
STREP-tag II insertion point
B
INT-Ub
Ub
11 10 9 8 7 6 5 4 3 2 1 0 −1 ppm
C
6xHIS E1
UBCH5a
MBP HOIP RBR-C
INT-Ub
INT-Ub.ΔGG
ATP
kDa
M1
135
80
25
11
IB: Ub
6xHIS E1
UBCH7
NleL
INT-Ub
INT-Ub.ΔGG
ATP
kDa
K6
135
80
25
11
IB: Ub
6xHIS E1
UBE2S-UBD
INT-Ub
INT-Ub.ΔGG
ATP
GST AMSH
kDa
K11
135
80
25
11
IB: Ub
6xHIS E1
UBCH7
MBP PARKIN
INT-Ub
INT-Ub.ΔGG
ATP
kDa
K48
135
80
25
11
IB: Ub
6xHIS E1
UBCH5c
GST CBL RF
INT-Ub
INT-Ub.ΔGG
ATP
kDa
K63
135
80
25
11
IB: Ub
6xHIS E1
6xHIS UBC13/UEV1
MBP PARKIN
INT-Ub
INT-Ub.ΔGG
ATP
kDa
K63
135
80
25
11
IB: Ub
D
INT-diUb
GST
GST UBAN, ABIN-1
GST UBAN, NEMO
GST UBAN, OPTN
kDa
22
IB: Ub
135
80
25
11
Ponceau S
E
INT-diUb
6xHIS USP2-cc
0
15
time [min]
kDa
20
11
IB: Ub
F
INT-diUb
OTULIN
0
15
time [min]
kDa
20
11
IB: Ub

# Figure 2.

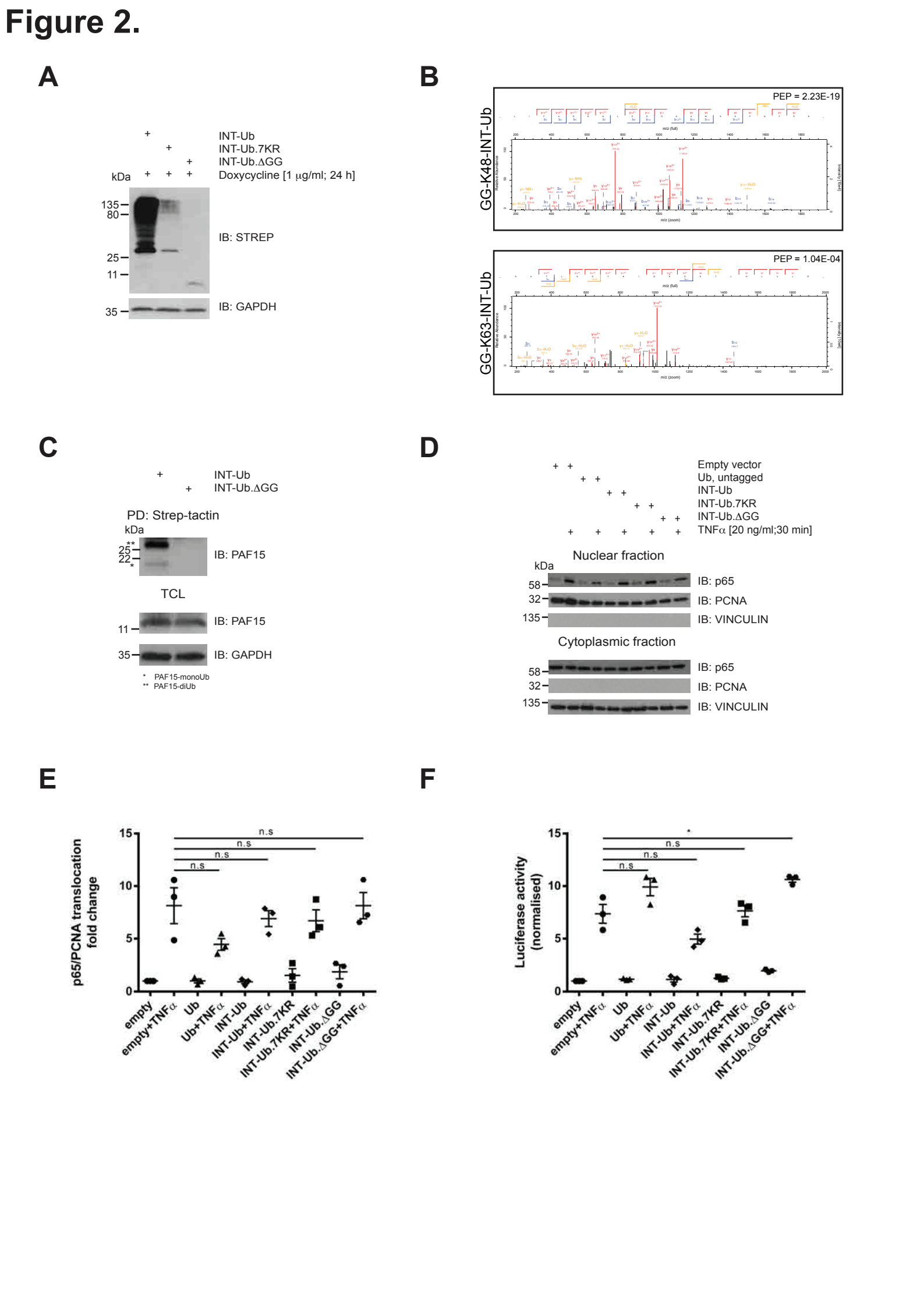
A
INT-Ub
INT-Ub.7KR
INT-Ub.ΔGG
kDa
Doxycycline [1 μg/ml; 24 h]
135
80
25
11
IB: STREP
35
IB: GAPDH
B
GG-K48-INT-Ub
PEP = 2.23E-19
GG-K63-INT-Ub
PEP = 1.04E-04
C
INT-Ub
INT-Ub.ΔGG
PD: Strep-tactin
kDa
25
22
IB: PAF15
TCL
11
IB: PAF15
35
IB: GAPDH
* PAF15-monoUb
** PAF15-diUb
D
Empty vector
Ub, untagged
INT-Ub
INT-Ub.7KR
INT-Ub.ΔGG
TNFα [20 ng/ml;30 min]
Nuclear fraction
kDa
58
IB: p65
32
IB: PCNA
135
IB: VINCULIN
Cytoplasmic fraction
58
IB: p65
32
IB: PCNA
135
IB: VINCULIN
E
p65/PCNA translocation fold change
n.s
empty
empty+TNFα
Ub
Ub+TNFα
INT-Ub
INT-Ub+TNFα
INT-Ub.7KR
INT-Ub.7KR+TNFα
INT-Ub.ΔGG
INT-Ub.ΔGG+TNFα
F
Luciferase activity (normalised)
*
n.s

# Figure 3.

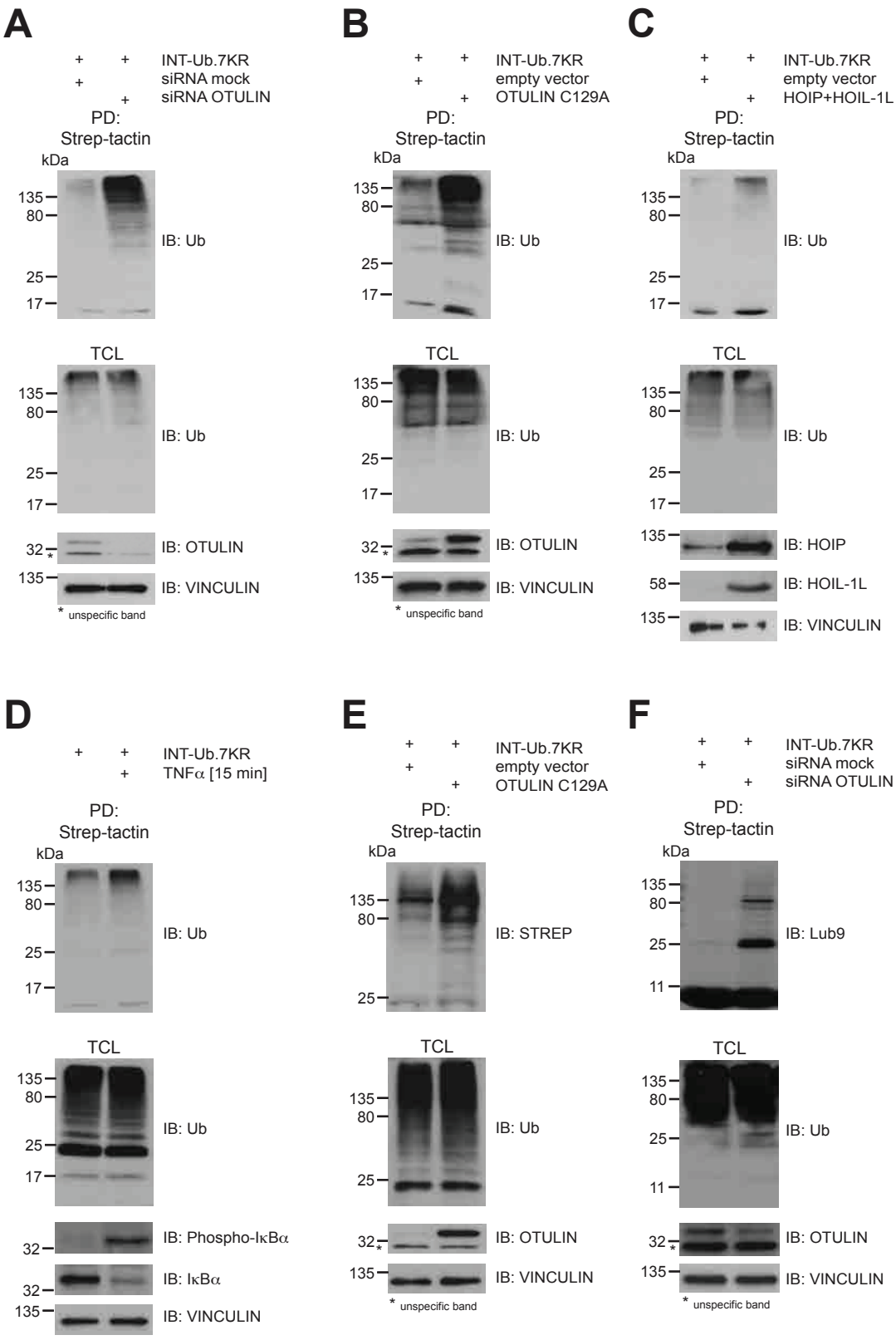
A
+ + INT-Ub.7KR
+ siRNA mock
+ siRNA OTULIN
PD: Strep-tactin
kDa
135
80
25
17
IB: Ub
TCL
135
80
25
17
IB: Ub
32
*
IB: OTULIN
135
IB: VINCULIN
* unspecific band
B
+ + INT-Ub.7KR
+ empty vector
+ OTULIN C129A
PD: Strep-tactin
kDa
135
80
25
17
IB: Ub
TCL
135
80
25
17
IB: Ub
32
*
IB: OTULIN
135
IB: VINCULIN
* unspecific band
C
+ + INT-Ub.7KR
+ empty vector
+ HOIP+HOIL-1L
PD: Strep-tactin
kDa
135
80
25
17
IB: Ub
TCL
135
80
25
17
IB: Ub
135
IB: HOIP
58
IB: HOIL-1L
135
IB: VINCULIN
D
+ + INT-Ub.7KR
+ TNFα [15 min]
PD: Strep-tactin
kDa
135
80
25
17
IB: Ub
TCL
135
80
25
17
IB: Ub
32
IB: Phospho-IκBα
32
IB: IκBα
135
IB: VINCULIN
E
+ + INT-Ub.7KR
+ empty vector
+ OTULIN C129A
PD: Strep-tactin
kDa
135
80
25
IB: STREP
TCL
135
80
25
IB: Ub
32
*
IB: OTULIN
135
IB: VINCULIN
* unspecific band
F
+ + INT-Ub.7KR
+ siRNA mock
+ siRNA OTULIN
PD: Strep-tactin
kDa
135
80
25
11
IB: Lub9
TCL
135
80
25
11
IB: Ub
32
*
IB: OTULIN
135
IB: VINCULIN
* unspecific band

# Figure 4.

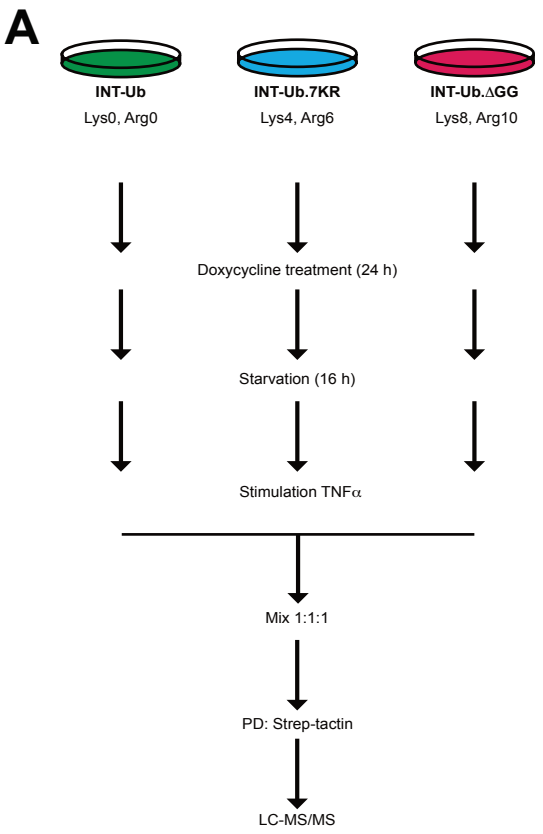


B

| Pathway | Enrichment factor | p value | Benj. Hoch. FDR | $-\log_{10}(p)$ |
|---|---|---|---|---|
| Ubiquitin mediated proteolysis | 9.7562 | 1.46E-17 | 6.70E-15 | 14.2 |
| Parkinson´s disease | 5.9621 | 8.13E-05 | 1.86E-02 | 1.7 |
| Systemic lupus erythematosus | 7.3006 | 3.24E-04 | 4.94E-02 | 1.3 |

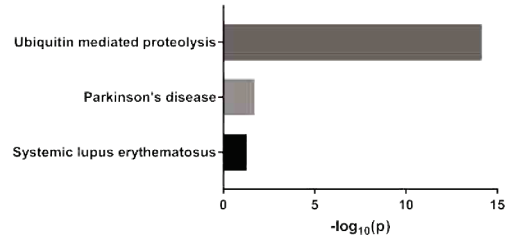


C

| Molecular function | Enrichment factor | p value | Benj. Hoch. FDR | $-\log_{10}(p)$ |
|---|---|---|---|---|
| ubiquitin-protein ligase activity | 9.6196 | 6.74E-20 | 1.94E-16 | 15.7 |
| small conjugating protein ligase activity | 9.2566 | 2.13E-19 | 3.06E-16 | 15.5 |
| acid-amino acid ligase activity | 8.9200 | 6.34E-19 | 6.07E-16 | 15.2 |
| ligase activity, forming carbon-nitrogen bonds | 7.7026 | 1.42E-18 | 1.02E-15 | 14.9 |
| ligase activity | 5.5402 | 2.87E-16 | 1.65E-13 | 12.7 |
| ubiquitin-protein ligase activity | 9.6196 | 6.74E-20 | 1.94E-16 | 15.7 |
| small conjugating protein ligase activity | 9.2566 | 2.13E-19 | 3.06E-16 | 15.5 |
| acid-amino acid ligase activity | 8.9200 | 6.34E-19 | 6.07E-16 | 15.2 |

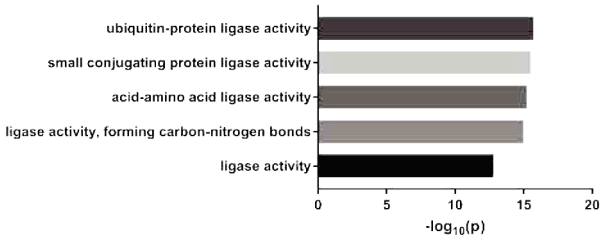


D

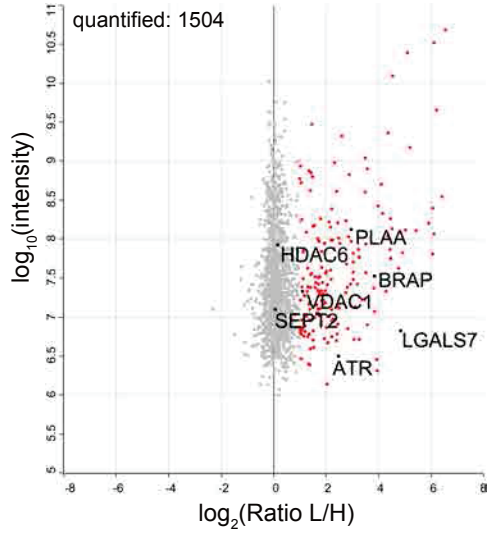


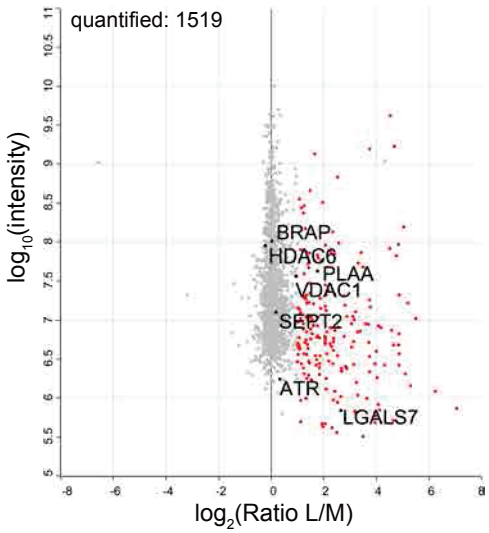


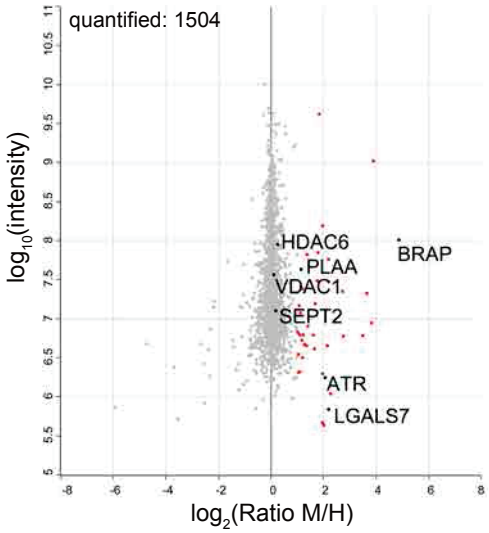

# Figure 5.

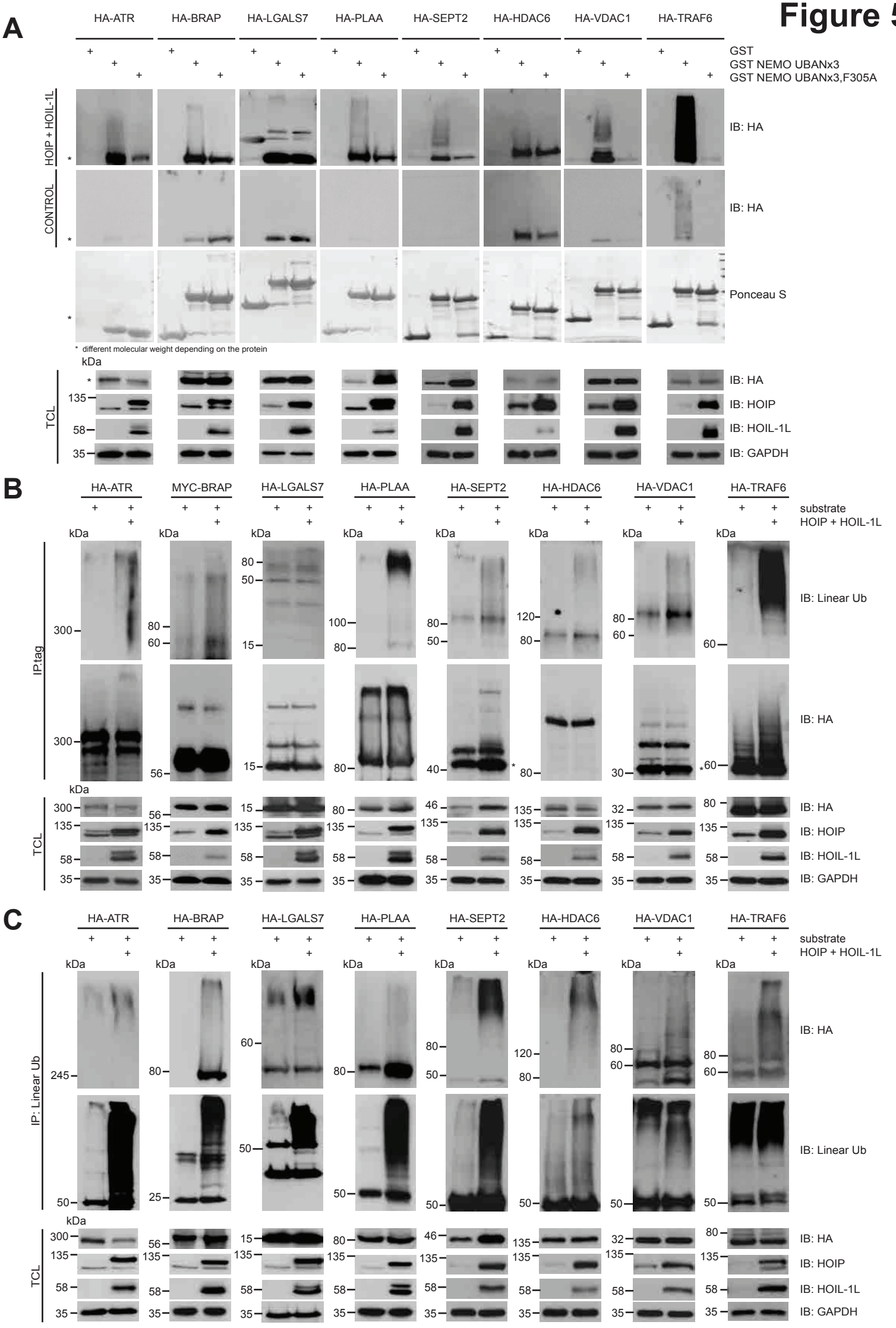
A
HA-ATR
HA-BRAP
HA-LGALS7
HA-PLAA
HA-SEPT2
HA-HDAC6
HA-VDAC1
HA-TRAF6
GST
GST NEMO UBANx3
GST NEMO UBANx3,F305A
HOIP + HOIL-1L
CONTROL
IB: HA
IB: HA
Ponceau S
* different molecular weight depending on the protein
kDa
TCL
IB: HA
IB: HOIP
IB: HOIL-1L
IB: GAPDH
B
HA-ATR
MYC-BRAP
HA-LGALS7
HA-PLAA
HA-SEPT2
HA-HDAC6
HA-VDAC1
HA-TRAF6
substrate
HOIP + HOIL-1L
IP:tag
IB: Linear Ub
IB: HA
TCL
IB: HA
IB: HOIP
IB: HOIL-1L
IB: GAPDH
C
HA-ATR
HA-BRAP
HA-LGALS7
HA-PLAA
HA-SEPT2
HA-HDAC6
HA-VDAC1
HA-TRAF6
substrate
HOIP + HOIL-1L
IP: Linear Ub
IB: HA
IB: Linear Ub
TCL
IB: HA
IB: HOIP
IB: HOIL-1L
IB: GAPDH

# Figure 6.

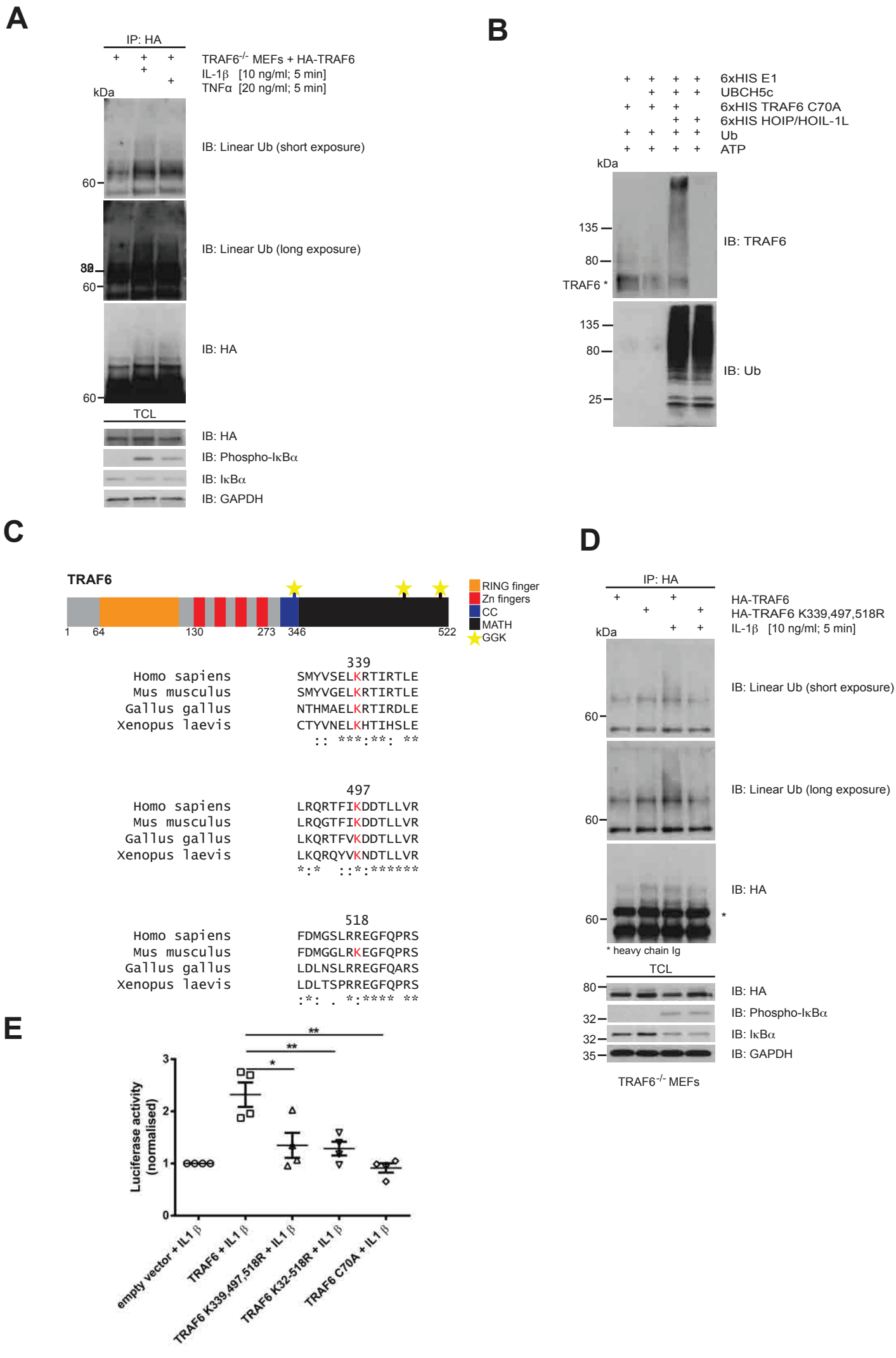
A
IP: HA
TRAF6-/- MEFs + HA-TRAF6
IL-1β [10 ng/ml; 5 min]
TNFα [20 ng/ml; 5 min]
kDa
IB: Linear Ub (short exposure)
IB: Linear Ub (long exposure)
IB: HA
TCL
IB: HA
IB: Phospho-IκBα
IB: IκBα
IB: GAPDH
B
6xHIS E1
UBCH5c
6xHIS TRAF6 C70A
6xHIS HOIP/HOIL-1L
Ub
ATP
IB: TRAF6
TRAF6 *
IB: Ub
C
TRAF6
RING finger
Zn fingers
CC
MATH
GGK
Homo sapiens SMYVSELKRTIRTLE
Mus musculus SMYVGELKRTIRTLE
Gallus gallus NTHMAELKRTIRDLE
Xenopus laevis CTYVNELKHTIHSLE
Homo sapiens LRQRTFIKDDTLLVR
Mus musculus LRQGTFIKDDTLLVR
Gallus gallus LKQRTFVKDDTLLVR
Xenopus laevis LKQRQYVKNDTLLVR
Homo sapiens FDMGSLRREGFQPRS
Mus musculus FDMGGLRKEGFQPRS
Gallus gallus LDLNSLRREGFQARS
Xenopus laevis LDLTSPRREGFQPRS
D
IP: HA
HA-TRAF6
HA-TRAF6 K339,497,518R
IL-1β [10 ng/ml; 5 min]
kDa
IB: Linear Ub (short exposure)
IB: Linear Ub (long exposure)
IB: HA
* heavy chain Ig
TCL
IB: HA
IB: Phospho-IκBα
IB: IκBα
IB: GAPDH
TRAF6-/- MEFs
E
Luciferase activity (normalised)
empty vector + IL1β
TRAF6 + IL1β
TRAF6 K339,497,518R + IL1β
TRAF6 K32-518R + IL1β
TRAF6 C70A + IL1β